Journal of Alloys and Compounds 509 (2011) 7047–7051

Contents lists available at ScienceDirect

Journal of Alloys and Compounds

journal homepage: www.elsevier.com/locate/jallcom

# Study of effect of covalency in heavy rare-earth monoantimonides upto 31 GPa

Sadhna Singh*, Purvee Bhardwaj

*High pressure Physics Lab., Department of Physics, Barkatullah University, Hoshangabad Road, Bhopal, M.P. 462026, India*

ARTICLE INFO

*Article history:*
Received 6 October 2010
Received in revised form 19 March 2011
Accepted 24 March 2011
Available online 1 April 2011

*PACS:*
62.20.de
62.20.dq
62.50.−p
64.00.00

*Keywords:*
Rare-earth alloy and compound
Phase transition
Crystal structure
Phase diagram
High pressure

ABSTRACT

In the present paper, we have investigated the high-pressure structural phase transition of rare earth antimonides (HoSb and TmSb). A modified interaction potential model (MIPM) (including the covalency effect) has been developed. Phase transition pressures are associated with a sudden collapse in volume. At compressed volumes, these compounds are found in CsCl phase. The phase transition pressures and associated volume collapses obtained from present potential model show a generally good agreement with available experimental data and others. The elastic constants and bulk modulus are also reported. Our results are in general in good agreement with experimental and theoretical data where available, and provide predictions where they are unavailable.



## 1. Introduction

Rare-earth monopnictides are generally semiconductors or semimetals. Despite their simple rock salt structure, they demonstrate various types of magnetic ordering generally with low transition temperatures. Their electronic structures and magnetic properties are sensitive to temperature, pressure and impurity effects. The rare-earth 4f–5d interactions and the hybridizations between the rare-earth non-4f and pnictogen p states are responsible for many fascinating phenomena that occur in rare-earth monopnictides [1]. Due to the unfilled 4f shells of rare-earth atoms, it is a challenging problem to obtain an accurate theoretical description of the electronic structure of rare-earth compounds [1–15]. In spite of the fact that the 4f energy levels often overlap with the non-4f broad bands of the system, they generally form very narrow resonances, and are often treated as core states in the theoretical efforts. Due to the highly localized nature of the 4f electrons, the direct f–f interactions between neighboring rare-earth atoms are generally considered to be nearly negligible. Among Nitride, Phosphide, Arsenide, Antimonide and Bismuthide there is gradual increase in metalicity in the rare-earth monopnictides. The typical carrier concentrations make them semimetals or highly doped n-type semiconductors [16].

The structural analysis under high pressure of rare earth monopnictides is important study. X-ray diffraction profile shows the NaCl type structure at ambient pressure and under pressure they show a B1–B2 type transition. In these transitions, the compression of the heavy rare earth atoms bring the 4*f* electrons into play so that these atoms behave more like the lighter rare earth elements. The rare earth element is less compressible than the other entity of these compounds so, pressure reduces the size of this entity more than it reduces the size of the rare earth. Relative sizes are thus restored to those prevailing for the lighter rare earths at atmospheric pressure.

Among the rare earth pnictides the rare earth antimonides (LnSb) have recently attracted particular interest as a proper reference material for understanding of various elastic, structural and magnetic effects [17–19]. Some of them show magnetic and crystallographic phase transitions at low temperatures. Monoantimonides with NaCl-type structure (CeSb, SmSb and YbSb), exhibit anomalies in various physical properties due to the p–f mixing, dense Kondo effect and heavy fermion state. For example, their carrier concentrations increase with decreasing temperature since the p–f mixing becomes stronger. On the other hand, other rare-earth monoantimonides behave as a nearly normal magnetic semimetal and display almost temperature-independent carrier concentrations [17–20].

* Corresponding author. Tel.: +91 755 2487552; fax: +91 755 2677723.
*E-mail addresses:* drsadhna100@gmail.com, drsadhna_in@rediffmail.com (S. Singh).

0925-8388/$ – see front matter © 2011 Elsevier B.V. All rights reserved.
doi:10.1016/j.jallcom.2011.03.139

Mullen et al. [2] studied the magnetic–lattice interaction for HoSb and TmSb. They concluded that the nature of this transition is complicated. For HoSb and TmSb they found that the structural and magnetic transitions coincide. Besides, the use of synchrotron radiation the powder X-ray diffraction of LnSb has systematically been studied up to 40 GPa at room temperature by Shirotani et al. [3,4]. The first order phase transition with the crystallographic change occurs for LnSb at high pressures. The structure of high pressure phases of LnSb is classified into three groups. The lighter LnSb (Ln = La, Ce, Pr, and Nd) have the tetragonal structure (distorted CsCl type) at high pressures. The high pressure form of the middle LnSb (Ln = Sm, Gd, and Tb) is unknown. The heavier LnSb (Ln = Dy, Ho, Er, Tm and Lu) show the typical NaCl–CsCl (B1–B2) transition at high pressures though the same transition is not observed in the heavier LnP and LnAs [3]. The transition pressures of LnSb increase with decreasing lattice constant in the NaCl type structure and do not depend on the structure of their high pressure phases. Magnetic properties of NdSb, GdSb, TbSb, DySb, HbSb and ErSb have been investigated by Missell et al. [21] under hydrostatic pressure. They concluded that the magnetic properties of DySb are strongly P-dependent, whereas those of HoSb are P-independent, but sample-dependent. Sapiro and Bak [22] studied the crystal field parameters and phase transitions in ErSb.

As we have already stated that the metallization in rare earth monopnictide increases from nitride to bismuthide, there is a need to include covalency effects for the study of these compounds. Looking at the interesting properties of these less explored rare earth antimonides and the fact that no work has been done with the potential model including covalecy effects, we thought it pertinent to apply a modified interaction potential model (MIPM) which includes the covalence effect in the potential model. The importance of covalence effect in rare earth monoantimonides has already been emphasized by Pagare et al. [23] and Vaitheeswaran et al. [12]. Vaitheeswaran et al. reported that their results on bulk moduli under high pressure is doubled which may be due to increase in covalent bonds. Pagare et al. [23] found discrepancy in their results on pressure derivatives of bulk moduli and they gave main reasons as partial covalent nature of these rare earth monoantimonides. Shirotoni et al. [24] has also confirmed the covalent character in chemical bond between atoms.

The present modified interaction potential model (MIPM) consists of Coulomb interaction, three body interactions, van der Waals interaction, overlap repulsive interaction and covalent interaction. The need of inclusion of three body interaction forces was emphasized by many workers for the better matching of results [25–27]. They concluded that possible reasons for disagreements include the failure of the two body potential model. Since these studies were based on two body potentials and could not explain Cauchy violations ($C_{12} \neq C_{44}$). They remarked that results could be improved by including the effect of non-rigidity of ions in the model. So three body interaction effects have been included in our potential model for the present study.

The purpose of this work is to provide some additional information to the existing data on the physical properties of two antimonides (HoSb and TmSb) theoretically. The main purpose of this work is to investigate the structural and elastic properties of HoSb and TmSb. The rest of this paper is organized as follows: the method of calculation is given in Section 2; the results and conclusion are presented and discussed in Section 3.

## 2. Potential model and method of calculation

The natural consequence of application of pressure on the crystals is the compression, which in turn leads to an increased charge transfer (or three-body interaction effects) [28] due to the existence of the deformed (or exchanged) charge between the overlapping electron shells of the adjacent ions.

These effects have been incorporated in the Gibbs free energy ($G = U+PV-TS$) as a function of pressure and three body interactions (TBI), which are the most dominant among the many body interactions. Here, $U$ is the internal energy of the system equivalent to the lattice energy at temperature near zero and $S$ is the entropy. At temperature $T = 0$ K and pressure ($P$) the

$$G_{BX}(r) = \frac{-\alpha_M^X Z^2 e^2}{r^X} - \frac{12\alpha_M^X Z e^2 f_m(r)}{r^X} - \left[\frac{C^X}{r^{X6}} + \frac{D^X}{r^{X8}}\right] + 6b\beta_{ij} \exp\left[\frac{r_i + r_j - r^X}{\rho}\right] + 6b\beta_{ii} \exp\left[\frac{2r_i - Y_X r^X}{\rho}\right] + 6b\beta_{jj} \exp\left[\frac{2r_j - Y_X r^X}{\rho}\right] + PV_{BX}(r^X) \quad (1)$$

where $X = 1$ (Phase 1 = B1), 2(Phase 2 = B2), and $Y_x = 1.414, 1.154$, for NaCl and CsCl structure respectively.

With $\alpha_m^X$ (where $X = 1$ (Phase 1 = B1), 2(Phase 2 = B2)) as the Madelung constant. $C$ and $D$ are the overall van der Waal coefficients for NaCl and CsCl structure respectively, $\beta_{ij}$ ($i,j = 1,2$) are the Pauling coefficients defined as $\beta_{ij} = 1+(Z_i/n_i)+(Z_j/n_j)$ with $Z_i$ ($Z_j$) and $n_i$ ($n_j$) as the valence and the number of electrons of the $i(j)$th ion. $Ze$ is the ionic charge and $b$ ($\rho$) are the hardness (range) parameters, $r$ is the nearest neighbour separations $f_m(r)$ is the modified three body force parameter which includes the covalency effect with three body interaction, $r_i$ ($r_j$) are the ionic radii of ions $i$ ($j$).

These lattice energies consist of long range Coulomb energy (first term), three body interactions corresponding to the nearest neighbour separation r modified by including covalency effect (second term), vdW (van der Waal) interaction (third term), energy due to the overlap repulsion represented by Hafemeister and Flygare (HF) type potential [29] and extended up to the second neighbour ions (fourth, fifth and sixth terms).

Covalency effects have been included in the second term in TBI parameter of cohesive energies given by Eq. (1) on the lines of Motida [30].

In the present model $f(r)$ is assumed to be constructed by two parts i.e.

1. due to covalency $f_{cov(r)}$
2. due to overlap distortion effect (three-body) $f_{TBI}(r)$

Now modified three body parameter $f_m(r)$ becomes

$$f_m(r) = f_{TBI}(r) + f_{Cov}(r) \quad (2)$$

where $f_{TBI}(r)$ is determined by the equation $f_{TBI}(r) = fe^{-r/}\rho$ here $\rho$ is the range parameter. The $f(r)$ due to covalency ($f_{cov}$) is given by

$$f_{\mathrm{cov}}(r) = \frac{4V_{sp\sigma}^2 e^2}{rE_g^3}$$

$$\frac{V_{sp\sigma}^2}{E_g^2} = \frac{1 - e_s^*}{12}$$

$$E_g = E - I + \frac{(2\alpha - 1)e^2}{r} \quad (3)$$

With $V_{sp\sigma}$ is the transfer matrix between the outer most $P$ orbital of anion and lowest excited state of cation $E_g$ is the transfer energy of electron from anion to cation. Denoting the static and optical

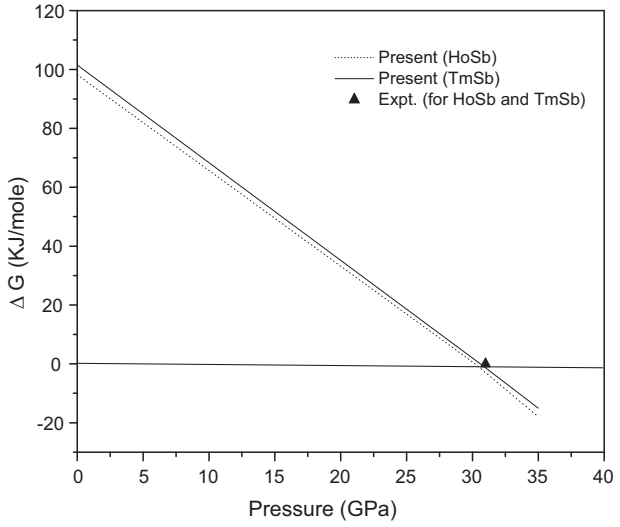


**Fig. 1.** Variation of Gibb's free energy with pressure for HoSb and TmSb.

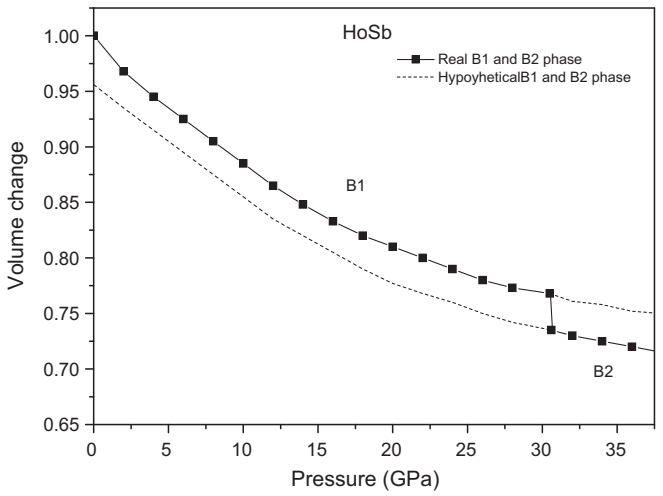


**Fig. 2.** Variation of volume change $V_P/V_0$ with pressure for HoSb, solid line + solid circles.

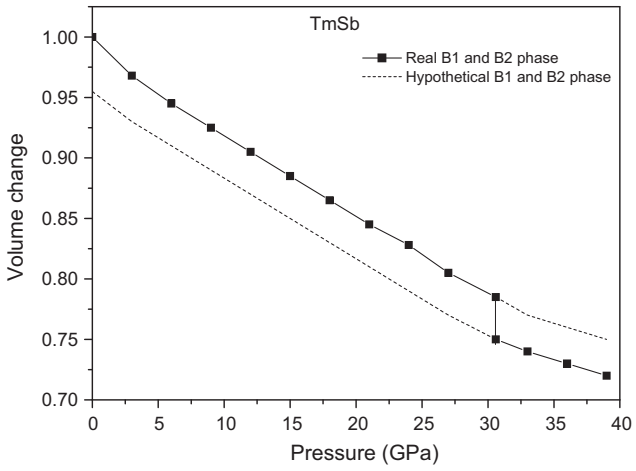


**Fig. 3.** Variation of volume change $V_P/V_0$ with pressure for TmSb.

dielectric constant $\varepsilon_0$ and $\varepsilon$, respectively and the transverse optical phonon frequency at zone centre by $\omega_t$, $e_s$ represented as

$$(e_s^*)^2 = \frac{9\mu\omega_t{}^2(\varepsilon_0 - \varepsilon_\infty)}{4\pi N(\varepsilon_\infty + 2)^2} \quad \text{and} \quad \frac{(e_s^*)^2}{(e)^2} = \frac{9\nu\mu\omega_0{}^2(\varepsilon_0 - \varepsilon_\infty)}{4\pi e^2(\varepsilon_\infty + 2)^2} \qquad (4)$$

where $\nu$ denotes the unit cell volume: $2r^3$, $r$ equilibrium value of the separation of the nearest neighboring ions, $\varepsilon_0$ the static dielectric constants, $\mu$ reduced mass of the ions, and $\omega_0$ the infrared dispersion frequency.

### 2.1. Structural properties

The B1 (NaCl) structure is most stable in these compounds and at high pressure they transform to body centered B2 (CsCl) structure. As, the stable phase is associated with minimum free energy of the crystal, we have followed the technique of minimization of Gibbs free energies of real and hypothetical phases. The phase transition occurs when $\Delta G$ approaches zero ($\Delta G \to 0$). At phase transition pressure ($P_t$) these compounds undergo a (B1–B2) transition associated with a sudden collapse in volume showing a first order phase transition.

We have also computed the relative volume changes $V(P)/V(0)$ corresponding to the values of $r$ and $r'$ at different pressures and plotted them against the pressure in Figs. 2 and 3 for HoSb and TmSb. It is clear from Table 2 and Figs. 2 and 3 that our calculated volume collapses $-\Delta V_{(p)}/V_{(0)}$ from our MIPM model for HoSb is 4.98%. The "−" sign shows the compression in crystal.

### 2.2. Elastic properties

We have applied the lattice theoretical study of second order elastic constants of cubic crystals by the method of homogeneous finite deformation. The potential is independent of temperature and entropy, so the mechanical elastic constants depend only on the configuration of the crystal. The only condition is that the known potential must be in an analytical form, i.e. it must be a function of relative positions of the ions in the crystal. The knowledge of second order elastic constants (SOECs) and their pressure derivatives are important for the understanding of the interatomic force in solids. The expressions of second order elastic constants are given in our earlier works [31,32].

## 3. Results and discussion

The Gibb's free energies contain three model parameters [$b$, $\rho$, $f_m(r)$]. The values of these parameters have been evaluated using lattice parameter, the first space derivatives of the lattice energy

**Table 1**
Input data and generated model parameters for HoSb and TmSb.

| Solid | Input parameters | | | Model parameters | | | | |
|---|---|---|---|---|---|---|---|---|
| | $r_i$(Å) | $r_j$(Å) | $r_0$ (Å) | $b(10^{-12}$ ergs) | $\rho$(Å) | $f_m(r)$ | $C(10^{-60}$erg cm$^6$) | $D(10^{-76}$erg cm$^8$) |
| HoSb | 0.894[a] | 1.25[a] | 3.57[b] | 10.3899 | 0.325 | −0.0189 | 8036.294 | 2008.799 |
| *TmSb* | 0.869[a] | 1.25[a] | 3.46[b] | 9.5868 | 0.316 | −0.0183 | 7684.439 | 1910.633 |

[a] Ref. [35].
[b] Ref. [28].

**Table 2**
Phase transition and volume change of HoSb and TmSb.

| Solid | Phase transition pressure (GPa) | | Volume collapse % |
|---|---|---|---|
| | Present | Expt. | Present |
| HoSb | 30.5 | 31[a] | 4.96 |
| TmSb | 30.6 | 31[a] | 5.74 |

[a] Ref. [28].

($U$) and equilibrium condition [33,34] expressed as:

$$\left[\frac{dU}{dr}\right]_{r=r_0} = 0 \tag{5}$$

$$B_1 + B_2 = -1.165{Z_m}^2 \tag{6}$$

where ${Z_m}^2 = Z(Z + 12f_m(r))$ and after following method adopted earlier [30,31]. Using these model parameters and the minimization technique, phase transition pressures of rare earth antimonides have been computed. The input data [35] of the crystal and calculated model parameters are listed in Table 1. Fig. 1 shows our present computed phase transition pressure for B1–B2 structure transition in HoSb at 30.5 GPa, and TmSb at 30.6 GPa, respectively. The present phase transition pressures have been illustrated by arrows in Fig. 1 and have been listed in Table 2 with their experimental (31 GPa for both HoSb and TmSb). It is interesting to note from Table 2 and Fig. 1 that the phase transitions pressures ($P_t$), obtained from the MIPM model, are in general in closer agreement with experimental data [24].

At elevated pressures, the materials undergo structural phase transition associated with a sudden change in the arrangement of the atoms. The atoms are rearranged in new positions leading to a new structure. Experimentally one usually studies the relative volume changes associated with the compressions. The discontinuity in volume at the transition pressure is obtained from the phase diagram. The compression curves are plotted in Figs. 2 and 3 for HoSb and TmSb, respectively. The values of the volume collapses (%) are depicted in Table 2. Our results on volume collapse are close to available experimental and other results. It is clear that during the phase transition from NaCl to CsCl, the volume discontinuity in pressure volume phase diagram identifies the same trend as the other experimental approach. In Figs. 2 and 3, solid lines + symbols represent the real B1 and B2 phases, dash lines represent the hypothetical B1 and B2 phases. It is revealed from Figs. 2 and 3 that our potential model can effectively explain the high pressure behavior of these compounds.

We display the results for various rare earth antimonides for lattice constants with phase transition pressure. From Fig. 4 it is clearly seen that the phase transition pressures of all the rare earth antimonides increases with decreasing lattice constants. This decrease occurs with increasing atomic number. We have compared our (solid triangles) results with experimental data (solid squares) [24]. It is clear from Fig. 4 that our values generally show the same trend as experimental results [24].

The study of elastic behavior under pressure is well known to supply useful information about change in the character of the covalent and ionic forces induced in the crystal as it is subjected to the phase transformation. We have calculated the second order elastic constants of the materials under study. Also, we could reproduce the correct sign of the elastic constants ($C_{11}$–$C_{12}$). The study of SOECs under pressure is important as $C_{11}$ represents elasticity in length and $C_{12}$ and $C_{44}$ are shape related elastic constants. The SOECs of rare earth antimonides have also been calculated and they are given in Table 3. The values of second order elastic constants given by Mullen et al. [2] at 200 K. Due to lack of experimental data for SOECs, we have compared our results with theoretical data but the values of SOECs are of the same order as reported by others

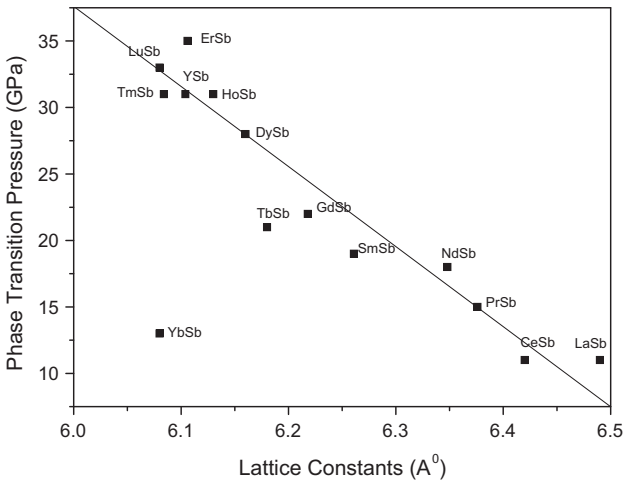


**Fig. 4.** Variation of lattice constant (a) with phase transition pressure for various rare earth antimonides.

**Table 3**
Calculated values of elastic constants (in GPa) and bulk modulus (in GPa) of HoSb and TmSb.

| Solid | HoSb | | TmSb | |
|---|---|---|---|---|
| | Present | Others | Present | Others |
| $C_{11}$ (GPa) | 98.56 | – | 102.69 | – |
| $C_{12}$ (GPa) | 17.65 | – | 20.54 | – |
| $C_{44}$ (GPa) | 21.32 | 27.6[a] | 24.81 | 26.8[a] |
| $C_{11}$–$C_{12}$ (GPa) | 80.91 | 138.0[a] | 82.15 | 135.0[a] |
| $B$ (GPa) | 44.62 | – | 47.92 | – |
| $\delta$ (GPa) | −3.67 | – | −4.27 | – |
| $\theta_D$ (K) | 279 | 247[a] | 258 | 237[a] |

[a] Ref. [2] (at 200° K).

[2]. To the best of our knowledge no experimental data of second order elastic constants for these rare earth antimonides have been reported yet.

Moreover, our present model is able to explain the Cauchy violation. One common approach is to assume that the atoms are connected with springs and that the resulting forces are only in the direction of the nearest neighbors (central force model). The deviation from the Cauchy violation $\delta = C_{12} - C_{44} - 2P$ is a measure of the contribution from the non central many-body force. The calculated values of Cauchy violation have been given in Table 3 for HoSb and TmSb.

In order to understand the thermo physical properties we have calculated the Debye temperature. The Debye characteristic temperature $\theta_D$ reflects its structure stability, the strength of bonds between its separate elements, structure defects availability and its density. The calculated values of elastic constants and Debye temperature for HoSb and TmSb have been listed in Table 3. Only the theoretical values are available for Debye temperature for HoSb and TmSb. Our values of Debye temperature of rare earth antimonides show the same trend as reported by Mullen et al. [2].

An overall assessment shows that in general, our values are near to available experimental data and they are in general better matching than other theoretical data. The success achieved in the present investigation can be ascribed to the inclusion of the covalency effect and charge transfer (or three body) as they seem to be of great importance at high pressure when the inter-ionic separation reduces considerably and the coordination number increases. The successful predictions achieved from the present model in the present compounds can be considered remarkable in view of the fact that it has considered overlap repulsion effective up to second neighbour ions.

Finally, it may be concluded that the present modified interaction potential model (MIPM) has successfully predicted the compression curves and phase diagrams giving the phase transition pressures, associated volume collapses and elastic properties correctly for these rare earth antimonides. The inclusion of three body interactions with covalency effect has improved the prediction of phase transition pressures over that obtained from the two-body potential and TBI without covalency. The use of suitable functional form for three body force parameter with covalency $f_m(r)$, instead of using it as a structure independent model parameter, might have improved the usefulness of the present model for estimating the actual high pressure behavior of the present compounds. Our results where no theoretical and experimental results are available may be tested with different theoretical and experimental and methods and may be taken as guide to future work.

## Acknowledgement

One of the authors (PB) is grateful to the Department of Science & Technology (DST), New Delhi for awarding WOS-'A' and the financial support to this work.

## References

[1] Chun-Gang Duan, R.F. Sabirianov, W.N. Mei, P.A. Dowben, S.S. Jaswal, E.Y. Tsymbal, J. Phys. Condens. Matter 19 (2007) 315220.
[2] M.E. Mullen, B. Luthi, P.S. Wang, Phys. Rev. B 10 (1974) 186–199.
[3] I. Shirotani, K. Yamanashi, J. Hayashi, O. Shimomura, T. Kikegawa, Solid. State. Commun. 127 (2003) 573–576.
[4] I. Shirotani, K. Yamanashi, J. Hayashi, Y. Tanaka, N. Ishimatsu, O. Shimomura, T. Kikegawa, J. Phys. Condens. Matter. 13 (2001) 1939–2019.
[5] H.M. Tutuncti, S. Bagci, G.P. Srivastava, J. Phys. Condens. Matter 19 (2007) 156207–156215.
[6] T. Adachi, I. Shirotani, J. Hayashi, O. Shimomura, Phys. Lett. A 250 (1998) 389–393.
[7] J. Hayashi, I. Shirotani, Y. Tanaka, T. Adachi, O. Shimomura, T. Kikegawa, Solid. State. Commun. 114 (2000) 561–576.
[8] U. Benedict, J. Alloys. Compd. 193 (1993) 88–93.
[9] J.C. Duthei, D.P. Pettifor, Phys. Rev. Lett. 38 (1977) 564–567.
[10] B. Luthi, M.E. Mullen, E. Bucher, Phys. Rev. Lett. 31 (1973) 95–98.
[11] J.M. Leger, D. Ravot, J. Roshad Mignod, J. Phys. C Solid State Phys. 17 (1984) 4935–4943.
[12] G. Vaitheeswaran, V. Kanchana, M. Rajgopalan, Phys. B 315 (2002) 64–73.
[13] G. Vaitheeswaran, V. Kanchana, M. Rajgopalan, J. Alloys. Compd. 336 (2002) 46–52.
[14] E. Deligoy, K. Colakoglu, Y.O. Chiftci, H. Ozisik, J. Phys. Condens. Matter 19 (2007) 436204–436211.
[15] A. Hasegawa, J. Phys. C Solid State Phys. 13 (1980) 6147–6615.
[16] W.P.L. Lambrecht, Phys. Rev. B 62 (2000) 13538–13545.
[17] M. Sera, J. Magn. Magn. Mater. 31–34 (1983) 385–389.
[18] S. Ozeki, Y. Ohe, Y.S. Kwon, Y. Haga, O. Nakamura, T. Suzuki, T. Kasuya, Phys. B 171 (1991) 286–288.
[19] A. Oyamada, C. Ayache, T. Suzuki, J. Rossat-Mignod, T. Kasuya, J. Magn. Magn. Mater. 90&91 (1990) 443–448.
[20] D.X. Li, Y. Haga, Y.S. Kwon, H. Shida, T. Suzuki, S. Nimori, G. Kido, J. Magn. Magn. Mater. 1165 (1995) 140–144.
[21] F.P. Missell, R.P. Guertil, S. Foner, Solid State Commun. 23 (1977) 369–372.
[22] S.M. Shapiro, P. Bak, J. Phys. Chem. Solids 36 (1975) 579–581.
[23] G. Pagare, S.P. Sanyal, P.K. Jha, Indian J. Pure Appl. Phys. 45 (2007) 459–464.
[24] I. Shirotani, J. Hayashi, K. Yamanashi, Phys. Rev. B 64 (2001) 132101–141321.
[25] C.E. Sims, G.D. Barrera, N.L. Allan, Phys. Rev. B 57 (1998) 11164–11172.
[26] B.S. Rao, S.P. Sanyal, Phys. Status Solidi (b) 165 (1991) 369–375.
[27] S. Froyen, M.L. Cohen, J. Phys. C 19 (1983) 2623–2632.
[28] R.K. Singh, Phys. Rep. 85 (1982) 259–401.
[29] D.W. Hafemeister, W.H. Flygare, J. Chem. Phys. 43 (1965) 795.
[30] K. Motida, J. Phys. Soc. Jpn. 55 (1986) 1636–1645.
[31] (a) P. Bhardwaj, S. Singh, N.K. Gaur, Cetr. Euro. J. Phys. 6 (2) (2008) 223–229; (b) P. Bhardwaj, S. Singh, N.K. Gaur, Mat. Res. Bull. 44 (2009) 1366–1369; (c) P. Bhardwaj, S. Singh, Phys. B 406 (2011) 1615–1621.
[32] (a) R.K. Singh, S. Singh, Phys. Rev. B 39 (1989) 671–678; (b) R.K. Singh, S. Singh, Phys. Rev. B 45 (1992) 1019–1022.
[33] U.C. Sharma, M.P. Verma, Phys. Status Solidi (b) 102 (1980) 487–494.
[34] U.C. Sharma, Ph.D. Thesis, Agra University, Agra (1985).
[35] D.R. Lide (Ed.), Handbook of Chemistry and Physics, 12, CRC, 1995–1996, pp. 21–24.